Int. J. Electrochem. Sci., 12 **(2017)** 2618 – 2627, doi: 10.20964/2017.04.73

International Journal of
ELECTROCHEMICAL
SCIENCE
www.electrochemsci.org

Yolk-shell Co_3O_4-CoO/Carbon Composites for Lithium-Ion Batteries with Enhanced Electrochemical Properties

Gongrui Wang[1], *Yanshuang Meng*[1,2,*], *Lei Wang*[1], *Jun Xia*[1], *Fuliang Zhu*[1,2], *Yue Zhang*[3,*]

[1] School of Materials Science and Engineering, Lanzhou University of Technology, Lanzhou 730050, China
[2] State Key Laboratory of Advanced Processing and Recycling of Non-ferrous Metals, Lanzhou 730050, China
[3] Department of Mechanical and Industrial Engineering, Texas A&M University-Kingsville, Kingsville, Texas, 78363, USA
[*]E-mail: mengyanshuang@163.com, yue.zhang@tamuk.edu

Received: 5 January 2017 / *Accepted:* 24 February 2017 / *Published:* 12 March 2017

A novel yolk-shell structured Co_3O_4-CoO/Carbon (Co_3O_4-CoO/C) composite was prepared and applied as cathode active materials in lithium ion batteries. The composites were prepared through a facile copolymerization of ionic liquid and acrylonitrile, which were used as carbon sources, followed by carbonization. The yolk-shell structure of the composite endows the electrodes with excellent cycling performance due to improved electronic conductivity, reduced strain and depressed aggregation of active materials compared with bare Co_3O_4. Thus, the Co_3O_4-CoO/C composite showed a high reversible capacity and cycling life of 590 mAh·g^{-1} after 50 charge/discharge cycles at a current rate of 890 mAh·g^{-1}.

Keywords: Co_3O_4-CoO/Carbon Composites; Yolk-shell structure; Lithium-ion batteries

1. INTRODUCTION

Lithium-ion batteries (LIBs) have been identified as one of the most important energy storage device because of their many beneficial properties such as low self-discharge rate, high voltage platform, environmental friendliness and portability [1-4]. However, as their applications expand from small-scale portable electronics to largescale electronic vehicles, graphite, the common used anode material with a limited theoretical capacity (372mAh·g^{-1}), can no longer meet the requirements for high density energy devices [5]. Therefore, plenty of researches have been taken to find a substitution

for conventional carbon materials as new anode materials to improve the electrical energy density for LIBs[6].

Transition metal oxides, such as Fe_3O_4, Fe_2O_3, Co_3O_4, have attract numerous attentions due to their high theoretical capacity which is several times higher than that of traditional electrodes [7-10]. The spinel crystal structured Co_3O_4 in particularly possess high theoretical capacity (890 $mAh \cdot g^{-1}$), high electro-activity, natural abundance, environmental friendliness and easy processing, which makes it an efficient anode electrode material for LIBs[10-13]. Nevertheless, the wide application of the Co_3O_4 in electrode is hindered by its low electron transfer ability and huge volume change during lithiation and dislithiation process. [14, 15].

To overcome this bottleneck, many researches have been carried out and can be divided into four groups: (1) Nanocrystallization of Co_3O_4 particles, which introduces many void among Co_3O_4 particles, can increase the contacting area between the active materials and electrolyteand, therefore, shorten the diffusion distance of ions and electrons[16]. In addition, the nanocrystallization can also moderate the stress existing in the Co_3O_4 electrode during the lithiation and dislithiation process [17]. (2) Specialization morphologies of Co_3O_4 nano-materials can prevent the aggregation of nanoparticles and maintain the cycling stability of its nanostructure[18, 19], such as flower-like morphologies[20], hollow microspheres[21], nanorods[18], nanotubes[22, 23], nanocages[10], nanowires[24], network-like morphologies[25] and etc.. (3) Combination of Co_3O_4 with other materials can improve its electrical conductivity and ameliorate its volume change effectively during charge-discharge process[26, 27]. Carbon materials (such as graphite[28], carbon nanotubes[29-31], graphene[32, 33] and etc.) and metallic oxide materials (such as Fe_2O_3[27], NiO[34] and etc.) are the mainly used integrating materials. (4) Cladding carbon film on Co_3O_4 particles to form mechanical protection layer, which can also promote to form uniform conductive network and stable solid electrolyte interface (SEI) during cycling process [35].

Among all these methods, combining Co_3O_4 with carbon materials is the most promising method because it can not only facilitate the transmission of electron but also accommodate the volume changes[15, 36]. Jun Liu et al.[37] used glucose as carbon source to synthesized carbon-coated mono-dispersed Co_3O_4 porous and hollow nanoparticles by using an *in-situ* carbon-coating method. The as-prepared nano-composites exhibited high reversible capacity (1150 $mAh \cdot g^{-1}$ for the initial 20 cycles at the current of 0.25C), stable cycle life, and high energy efficiency (1078 $mAh \cdot g^{-1}$ at the current of 0.5C, 700 $mAh \cdot g^{-1}$ at the current of 2C). Baojun Li et al.[38] successfully prepared a Co_3O_4@graphene composites through a chemical deposition method, with Co_3O_4 nanoparticles homogeneously dispersed onto graphene sheets, displaying a superior cyclic performance in LIBs.

Among all the precursors of carbon films, ionic liquids (ILs) have been the focus of an ever increasing amount of research due to its extraordinary properties, such as negligible vapor pressure and structure designability. The negligible vapor of ILs enable them simple processing during the carbonization process without evaporation. In addition, as the ILs are designable, it is feasible to synthesis carbon materials with controllable structure and a certain amount of heteroatoms by adjusting the cation or anion components of ILs. Due to these unique properties, the integrating carbon film prepared from ILs show superior electronic conductivity, and excellent bonding strength between carbon substrate and active materials[39, 40].

In this study, Co_3O_4-CoO/C composites have been successfully synthesized by the polymerization of the hydroxide radicals on the surface of cobalt oxide, using IL and acrylonitrile as monomers, followed by carbonization of the above copolymers. The as-obtained composites exhibit a novel yolk-shell structure and an enhanced electrochemical performance when served as electrode materials. The electrodes made of the composites possess a superior cycling capacity of 580 $mAh \cdot g^{-1}$. Due to the facile preparation method, favorable capacity and outstanding cycling performance, the yolk-shell structured Co_3O_4-CoO/C composite is an promising candidate for electrode material of lithium ion batteries.

2. EXPERIMENTAL SECTION

2.1 Materials synthesis

Co_3O_4 (99%) was purchased from Aladdin. 1-vinyl-3-methyl tetrafluoroborate was purchased from Lanzhou Institute of Chemical Physics. All the other reagents were analytical grade and used without further purify. In a representative synthesis, 1g Co_3O_4 was added into the solution(84ml) of deionized water and absolute ethyl alcohol (1:1 by vol.%). Subsequently, 9 ml silane coupling agent (KH570) is dissolved dropwise into the above mixture with continuous stirring at ambient environment followed by ultrasonication for half an hour. The PH value of the mixture was then adjusted to 5 by acetic acid at room temperature. The mixture was mechanical stirred for an hour, heating in water bath at 30 ℃. The modified Co_3O_4 was separated by suction filtration and washed with deionized water for three times. The modified Co_3O_4 (0.5g) was mixed with the solution (40ml) of deionized water and absolute ethyl alcohol (1:1 by vol.%). 0.6g acrylonitrile (AN) , 0.4g ionic liquid (IL),0.07g 2,2-azobisisobutyronitrile (AIBN) and 0.1g poly(ethylene glycol) diacrylate (PEGDA) were added into the above mixture in sequence followed by mechanical stirring for 20 hours at ambient conditions. The obtained sample was washed with deionized water for 3 times, and finally, calcined for 2 hours at the temperature of 500 ℃ with the protection of argon atmosphere.

2.2 Materials characterization

The phase structure of as-prepared samples were characterized with X-ray diffraction (XRD, D/max-2400, Cu Kα).The morphology was studied by transmission electron microscope (TEM, JEM-1200EX, 100kV) and scanning electron microscope (SEM, Quanta450FEG). The presence of organic groups on the sample surface was analyzed by Fourier transform infrared spectroscopy (FTIR, Nexus 670). Raman spectra was conducted with excitation from the 532 nm line of an Ar ion laser on LabRAM HR800.

2.3 Electrochemical measurements

The electrochemical properties of as-synthesized materials were evaluated by using CR2032 type coin cells assembled in argon-filled glove box. The working electrodes were fabricated by

spreading the slurry on copper foils current collector, which was a mixture of 85 wt.% active materials (Co_3O_4-CoO/C or bare Co_3O_4), 8 wt.% acetylene black as conductive material, 7 wt.% polyvinylidene fluoride (PVDF). After that, the working electrodes were dried in vacuum at 60 ◦C for 6 hours and pressed subsequently. Lithium foil was employed as the counter electrode, and Celgard 2300 served as a separator. The electrolyte was a solution of 1.0M LiPF6 in ethylene carbonate (EC) and1,2-dimethoxyethane (DME) (1:1 by vol.%). The electrode capacity and cycling properties were measured by a galvanostatic discharge-charge method in the voltage range between 0.005 and 3.0V (vs. Li/Li^+) at a current density of 89 $mAh \cdot g^{-1}$ on a battery test system (LAND CT2001, China).

3. RESULTS AND DISCUSSION

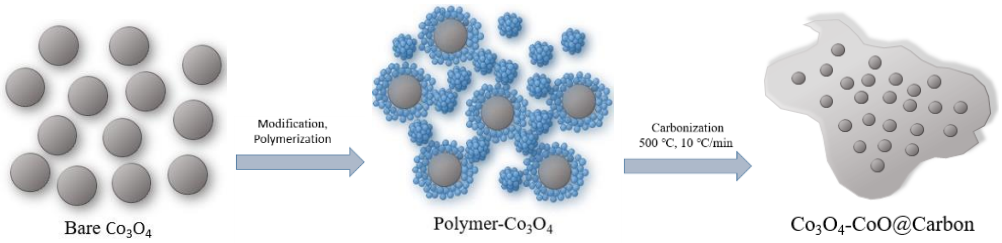

Figure 1. Schematic of the synthesis process for Co_3O_4-CoO/C composites.

The preparation process of Co_3O_4-CoO/C composites was depicted in Fig.1. In order to obtain the modified Co_3O_4, KH570 and acetic acid were added into a water-ethanol suspension of bare Co_3O_4 under uninterrupted stirring. To synthesis polymer-Co_3O_4 composites, the ionic liquid and acrylonitrile were mixed with the modified Co_3O_4 and water-ethanol solution followed by adding the other reagents with the existence of water bath, and after that, the mixture was stirred for twenty hours. The as-obtained polymer-Co_3O_4 were washed for three times, and then calcined at the argon atmosphere to obtain the Co_3O_4-CoO/C composites promoted by carbonization and reduction actions.

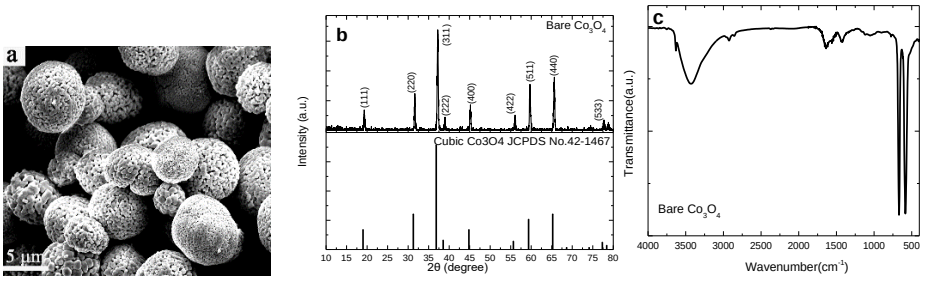

Figure 2. SEM image (a), X-ray diffraction patterns (b), and FTIR spectrum (c) of bare Co_3O_4

The surface morphology of bare Co_3O_4 micro-particles has been investigated by using Scanning Electron microscope (SEM), as seen in Fig.2a. The bare Co_3O_4 are uniform spherical mono-

particles composed of nano-grains with numerous pores. Fig.2b shows the representative x-ray diffraction (XRD) patterns of spinel structured Co_3O_4. The diffraction reflections of bare Co_3O_4 at 2θ=19.1, 31.6°, 37.2°, 38.8°, 45.3°, 56.1°, 59.8°, 65.6°and 77.8° are attributed to (111)，(220)，(311)，(222)，(400)，(422)，(511)，(440) and (533) planes, respectively, implying the well crystallization of the as-mentioned bare Co_3O_4 with spinel structure. The strong and sharp peaks of spherical Co_3O_4 proved its well formation at the same time.

FTIR spectrum of bare Co_3O_4 (fig.2c) showed two characteristic absorption peaks at 566cm^{-1} and 671cm^{-1} verify the existence of spinel structured Co_3O_4[41].The band at 566cm^{-1} indicates that the OB_3 composition of the spinel structure, where B refers to Co^{3+} in the octahedral interstice, and the band at 671cm^{-1} implies the ABO_3 composition of the spinel structure, where A denotes Co^{2+} in the tetrahedron interstice and B refers to Co^{3+} in the octahedral interstice[42, 43].The absorption peaks at 3430 cm^{-1} and 1637 cm^{-1} are ascribed to –OH of water existed in samples or KBr[44].The unsharp peak at 3632cm^{-1} is attributed to the non-hydrogen bond O–H[45], which confirms the hydroxide radicals are on the cobalt oxide micro-particles.

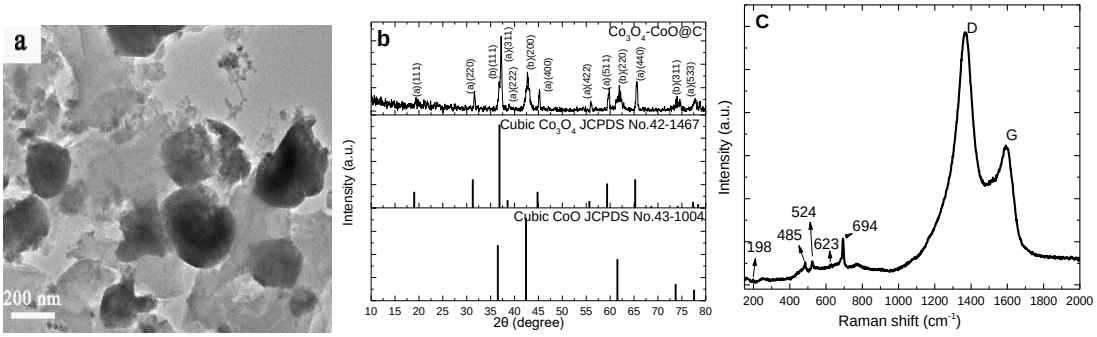

Figure 3. TEM image (a), X-Ray diffraction pattern (b), and Raman spectrum (c) of Co3O4-CoO/C

Fig.3a displays the morphology and microstructure of as-obtained Co_3O_4-CoO/C composites by using TEM analysis. We can observe cobalt oxide particles seeding in the carbonous substrate uniformly. The interface between cobalt oxide and nitrogen doped carbon bonds well, which is beneficial for the transmission of electrons. The morphology of cobalt oxide particles, after annealing, have changed into irregular spherical particles by comparison with bare Co_3O_4 (fig.2a). There are grains incorporated with each other on account of calcinating and agglomerating effects. It is distinctive that the particle size is smaller than bare Co_3O_4, from which it can be deduced that it is aroused by the emitting of oxygen atoms from Co_3O_4 and the collapsing of the Co_3O_4 particles.

Apparently, a crucial transformation of the as-synthesized composites has taken place compared with bare Co_3O_4 (fig.2b) as revealed by XRD diffraction patterns (fig.3b),demonstrating that the initial bare Co_3O_4 with spinel structure has partially changed into face-centered cubic structured CoO aroused by the reduction action of polyacrylonitrile (PAN) and poly ionic liquid (PIL). The diffraction peaks at 2θ=19.1°, 31.6°, 37.2°, 38.8°, 45.3°, 56.1°, 59.8°, 65.6°and 77.8° are corresponded to (111)，(220)，(311)，(222)，(400)，(422)，(511)，(440) and (533) planes of spinel structured Co_3O_4, respectively. The diffraction peaks at 2θ=36.8, 42.6, 61.6 and 74.3 are assigned to (111), (200),

(220) and (311) planes of face-centered cubic structured CoO, respectively. Meanwhile, it is worthy to take note of that the main phase is spinel structured Co_3O_4, mixed with relatively less CoO phase as designed.

The Raman spectra of the composites was shown in Fig.3c. The peaks at 1365 cm^{-1} and 1592 cm^{-1} are attributed to D band and G band respectively[46, 47]. The D band corresponds to the vibration of sp^3-hybridization carbon originating from the defects of the carbon substrates, and the G band is ascribed to the vibration of sp^2-hybridization carbon which is related with graphitic carbon[48, 49]. The intensity ratio of D and G bands (I_D/I_G) is widely applied to characterize the graphitization degree of carbon materials or the carbon disorder degree[50, 51]. The I_D/I_G value was found to be 1.30, indicated that the carbon substrates have a high disorder degree. The peaks around 198 cm^{-1}, 485 cm^{-1}, 524 cm^{-1}, 623 cm^{-1}, 694 cm^{-1} correspond to the B_{1g}, E_g, F^1_{2g}, F^2_{2g} and A_{1g} modes of Co_3O_4, respectively[50, 52]. Whereas, due to the limited amount of CoO, its characteristic peak is barely observed[47].

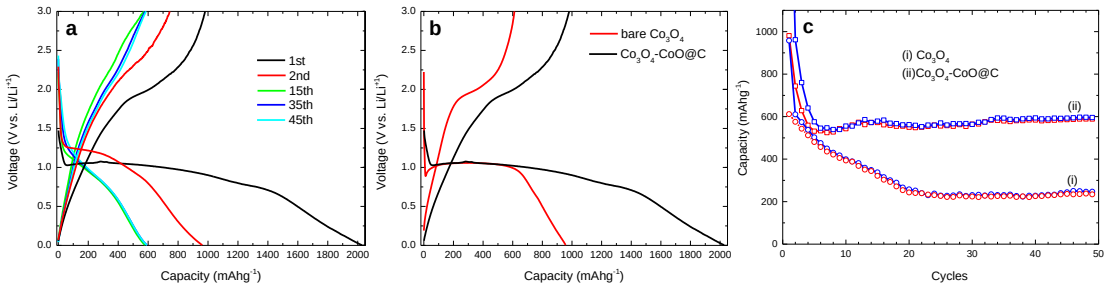

Figure 4. Electrochemical performance. a) the first charge-discharge voltage profiles of bare Co_3O_4 and Co_3O_4-CoO/C composites, respectively. b) the discharge-charge voltage profiles of Co_3O_4-CoO/C composites. c) cycling performance of bare Co_3O_4 and Co_3O_4-CoO/C composites, respectively.

The discharge-charge voltage profiles, at a current density of 89 $mAh \cdot g^{-1}$, of the electrodes made of as-obtained Co_3O_4-CoO/C composites are exhibited in fig.4a. The first long discharge voltage plateau, with a classic feature, at about 1.05V can be witnessed, assigning to the formation of solid electrolyte interfaces (SEI) and the transformation of cobalt oxide to cobalt[53].The first charge voltage plateau at about 1.9V can be attributed to the oxidation reaction of cobalt to cobalt oxide[30]. When it comes to the second discharge process, the voltage plateau becomes more gradient, which is imputed to the heterogeneity of the active materials during lithiation and dislithiation[1]. Satisfactorily, the 35^{th} and 45^{th} are in line with each other, implying the favorable reversibility of the composites.

Fig.4b shows the first discharge-charge voltage profiles of the electrode made of bare Co_3O_4 and the as-obtained composites, respectively. Unexpectedly, the first discharge capacity of the both materials have exceeded theoretical capacities, especially for the as-obtained composites, which are due to the decomposition of electrolyte and the formation of SEI layers[37]. As for the as-obtained composites, the especially large first discharge capacities might originate from the lower internal resistance (proved by a little lower discharge voltage plateau) [54] and the shortened the lithium ion

diffusion length of the smaller cobalt oxide particles (fig.3a) [31, 55, 56]. Moreover, the smaller particle size can also attribute in seriously decomposition of electrolyte.

As shown in fig.4c, The cycling performances of both electrodes have been measured at the current density of 89 $mAh \cdot g^{-1}$, indicating that the Co_3O_4-CoO/C electrode possesses a better performance. With regard to the Co_3O_4-CoO/C electrode, the reversible capacity declined up to the 10^{th} cycle, and increased slowly to about 580 $mAh \cdot g^{-1}$ due to the activation process of electrode materials or an ameliorative surface wetting performance of electrolyte[57, 58], subsequently showed a good capacity retention. For comparison, the bare Co_3O_4 electrode reversible capacity continues to decline until the 50^{th} cycle.

It has been reported that bare Co_3O_4 suffers from extremely large volume changes and particle agglomeration during the reduplicative lithiation and dislithiation which can also lead to the pulverization and exfoliation of the electrode due to the huge volume change, resulting in the on-going deterioration of the cell[43]. As for Co_3O_4-CoO/C electrode, the yolk-shell composites have improved electronic conductivity, with carbonous substrate facilitating the transmission of electron[59, 60]. Carbonous substrate can also avoid the aggregation of active materials and relieve the strain during lithium insertion and extraction[55], which is favorable for the prevention of the pulverization and exfoliation of the electrode, and beneficial for the maintenance of its cycling stability. All these reasons contribute to the excellent cycling performance.

The electrochemical performance of the Co_3O_4/C electrode is compared with previous studies as shown in Table 1. The as prepared composite displays competitive comprehensive electrochemical properties, implying that the composite has a promising prospect in the future.

Table 1. Comparison of the Co_3O_4/C electrode with similar electrodes reported in the literature

Material	Grain size	Morphology	Specific capacity ($mAh \cdot g^{-1}$)	Current density ($mA \cdot g^{-1}$)	Upgrade rate (%)	Cycle number	Ref.
Co_3O_4@C	Length 100nm Diameter 25nm	dendrite-like	500	89	238	40	35
Co_3O_4/C	10-20 nm	Co_3O_4/Carbon matrix	822	100	40.7	30	36
Co_3O_4/C	250 nm	quasi-sphere	1150	222	29.2	20	37
Co_3O_4@graphene	10-30 nm	CGC	740	178	270	60	38
Co_3O_4-CoO/C	~5 μm	Solid sphere	580	89	190	50	this work

4. CONCLUSION

In summary, the present work demonstrated a novel preparation approach of Co_3O_4-CoO/C composites via a copolymerization of ionic liquid and acrylonitrile followed by carbonization method. The structure and morphology analysis revealed that the composites have an excellent yolk-shell structure and the interface between cobalt oxide and carbonous substrate bonds well, which is responsible for the superior cycling performance. In order to manifest the tremendous superiority, bare Co_3O_4 electrodes were also fabricated, of which the capacity continuous to decline up to 50 cycles. The excellent cycling performance of Co_3O_4-CoO/C composites is due to improved electronic conductivity, reduced strain and depressed aggregation of active materials. According to these results, we can conclude that the Co_3O_4-CoO/C composites have a promising prospect as a new-style electrode materials of lithium ion batteries.

CONFLICTS OF INTEREST STATEMENT

The authors certify that they have NO affiliations with or involvement in any organization or entity with any financial interest (such as honoraria; educational grants; participation in speakers' bureaus; membership, employment, consultancies, stock ownership, or other equity interest; and expert testimony or patent-licensing arrangements), or non-financial interest (such as personal or professional relationships, affiliations, knowledge or beliefs) in the subject matter or materials discussed in this manuscript.

ACKNOWLEDGEMENT

The project was supported by the National Natural Science Foundation of China (grant No. 51364024, 51404124), Natural Science Foundation of Gansu Province (grant No. 1506RJZA100), Research and Development Fund of Lanzhou University of Technology (01-0443).

References

1. X.J. Lv, Z.M. Xu, J. Li, J.G. Chen, Q.S. Liu, *Journal of Alloys and Compounds*, 681 (2016)253.
2. J.M. Won, J.S. Cho, Y.C. Kang, *Journal of Alloys and Compounds*, 680 (2016)366.
3. L.M. Zhang, X.B. Wang, S. Tao, G.X. Wu, X.Z. Su, S.Q. Wei, H.F. Zhao, W.S. Chu, *Mater Lett*, 179 (2016)34.
4. W. Li, K. Shang, Y. Liu, Y. Zhu, R. Zeng, L. Zhao, Y. Wu, L. Li, Y. Chu, J. Liang, G. Liu, *Electrochim Acta*, 174 (2015)985.
5. J.S. Kim, W. Choi, K.Y. Cho, D. Byun, J. Lim, J.K. Lee, *J Power Sources*, 244 (2013)521.
6. Z. Yuan, F. Huang, C. Feng, J. Sun, Y. Zhou, *Materials Chemistry and Physics* (2003)4.
7. F. Cheng, K. Huang, S. Liu, J. Liu, R. Deng, *Electrochim Acta*, 56 (2011)5593.
8. Y. Liu, A.A. Elzatahry, W. Luo, K. Lan, P. Zhang, J. Fan, Y. Wei, C. Wang, Y. Deng, G. Zheng, F. Zhang, Y. Tang, L. Mai, D. Zhao, *Nano Energy*, 25 (2016)80.
9. L. Yang, G. Guo, H. Sun, X. Shen, J. Hu, A. Dong, D. Yang, *Electrochim Acta*, 190 (2016)797.
10. N. Yan, L. Hu, Y. Li, Y. Wang, H. Zhong, X. Hu, X. Kong, Q. Chen, *The Journal of Physical Chemistry C*, 116 (2012)7227.
11. Z.-Y. Li, P.T.M. Bui, D.-H. Kwak, M.S. Akhtar, O.B. Yang, *Ceramics International*, 42 (2016)1879.

12. X. Pan, X. Chen, Y. Li, Z. Yu, *Electrochim Acta*, 182 (2015)1101.
13. F. Wang, C. Lu, Y. Qin, C. Liang, M. Zhao, S. Yang, Z. Sun, X. Song, *J Power Sources*, 235 (2013)67.
14. C. Zhou, Y. Zhang, Y. Li, J. Liu, *Nano Lett*, 13 (2013)2078.
15. S.H. Yu, S.H. Lee, D.J. Lee, Y.E. Sung, T. Hyeon, *Small*, 12 (2016)2146.
16. D.W. Zhang, A. Qian, J.J. Chen, J.W. Wen, L. Wang, C.H. Chen, *Ionics*, 18 (2012)591.
17. B. Zhang, Y.B. Zhang, Z.Z. Miao, T.X. Wu, Z.D. Zhang, X.G. Yang, *J Power Sources*, 248 (2014)289.
18. R. Xu, J.W. Wang, Q.Y. Li, G.Y. Sun, E.B. Wang, S.H. Li, J.M. Gu, M.L. Ju, *J Solid State Chem*, 182 (2009)3177.
19. C.X. Zhang, S. Chen, J.Y. Zhan, Y.M. Shen, S.B. Zhou, C.G. Zuo, X.H. Xia, *Mater Technol*, 31 (2016)532.
20. J. Zheng, J. Liu, D.P. Lv, Q. Kuang, Z.Y. Jiang, Z.X. Xie, R.B. Huang, L.S. Zheng, *J Solid State Chem*, 183 (2010)600.
21. J.Y. Wang, N.L. Yang, H.J. Tang, Z.H. Dong, Q. Jin, M. Yang, D. Kisailus, H.J. Zhao, Z.Y. Tang, D. Wang, *Angew Chem Int Edit*, 52 (2013)6417.
22. Z.G. Yang, S.P. Wang, Y.C. Liu, X.R. Lei, *Ionics*, 21 (2015)2423.
23. Z.T. Cui, S.G. Wang, Y.H. Zhang, M.H. Cao, *Electrochim Acta*, 182 (2015)507.
24. H. Che, A. Liu, J. Hou, J. Mu, Y. Bai, S. Zhao, X. Zhang, H. He, *Journal of Materials Science: Materials in Electronics*, 25 (2014)3209.
25. X.X. Zhang, Q.S. Xie, G.H. Yue, Y. Zhang, X.Q. Zhang, A.L. Lu, D.L. Peng, *Electrochim Acta*, 111 (2013)746.
26. J.X. Wang, Q.B. Zhang, X.H. Li, D.G. Xu, Z.X. Wang, H.J. Guo, K.L. Zhang, *Nano Energy*, 6 (2014)19.
27. Q.Q. Xiong, X.H. Xia, J.P. Tu, J. Chen, Y.Q. Zhang, D. Zhou, C.D. Gu, X.L. Wang, *J Power Sources*, 240 (2013)344.
28. T.T. Jiang, Y. Wang, K. Wang, Y.R. Liang, D.C. Wu, P. Tsiakaras, S.Q. Song, *Appl Catal B-Environ*, 189 (2016)1.
29. Y.H. Xiao, S.J. Liu, S.M. Fang, D.Z. Jia, H.Q. Su, W.L. Zhou, J.B. Wiley, F. Li, *Rsc Advances*, 2 (2012)3496.
30. Y.M. Chen, L. Yu, X.W. Lou, *Angew Chem Int Ed Engl*, 55 (2016)5990.
31. N. Du, H. Zhang, B.D. Chen, J.B. Wu, X.Y. Ma, Z.H. Liu, Y.Q. Zhang, D.R. Yang, X.H. Huang, J.P. Tu, *Adv Mater*, 19 (2007)4505.
32. W.J. Zhu, H. Huang, Y.P. Gan, X.Y. Tao, Y. Xia, W.K. Zhang, *Electrochim Acta*, 138 (2014)376.
33. V.H. Nguyen, J.-J. Shim, *Mater Lett*, 157 (2015)290.
34. Y.P. Zhang, Q.Q. Zhuo, X.X. Lv, Y.Y. Ma, J. Zhong, X.H. Sun, *Electrochim Acta*, 178 (2015)590.
35. S.B. Zhou, G. Wang, Y.Z. Xie, H. Wang, J.B. Bai, *J Nanopart Res*, 15 (2013).
36. B.C. Yu, J.O. Lee, J.H. Song, C.M. Park, C.K. Lee, H.J. Sohn, *J Solid State Electr*, 16 (2012)2631.
37. J. Liu, Y. Wan, C. Liu, W. Liu, S. Ji, Y. Zhou, J. Wang, *Eur J Inorg Chem*, 2012 (2012)3825.
38. B. Li, H. Cao, J. Shao, G. Li, M. Qu, G. Yin, *Inorganic chemistry*, 50 (2011)1628.
39. Y.S. Meng, Z. Zhang, W.Q. Han, Y. Zhang, F.L. Zhu, D.J. Wang, *Nano*, 11 (2016).
40. Y.S. Meng, J. Xia, F.L. Zhu, Y. Zhang, *International Journal of Electrochemical Science*, 11 (2016)9881.
41. C. Nethravathi, S. Sen, N. Ravishankar, M. Rajamathi, C. Pietzonka, B. Harbrecht, *J. Phys. Chem.*, (2005).
42. D. Zhang, F. Li, A. Chen, Q. Xie, M. Wang, X. Zhang, S. Li, J. Gong, G. Han, A. Ying, Z. Tong, *Solid State Sciences*, 13 (2011)1221.
43. J. Byun, H.A. Patel, D.J. Kim, C.H. Jung, J.Y. Park, J.W. Choi, C.T. Yavuz, *J. Mater. Chem. A*, 3 (2015)15489.

44. L. Sun, H. Li, L. Ren, C. Hu, *Solid State Sciences*, 11 (2009)108.
45. X.-h. Xia, J.-p. Tu, Y.-j. Mai, X.-l. Wang, C.-d. Gu, X.-b. Zhao, *J Mater Chem*, 21 (2011)9319.
46. K. Wenelska, C. Neef, L. Schlestein, R. Klingeler, R.J. Kalenczuk, E. Mijowska, *Chem Phys Lett*, 635 (2015)185.
47. G. Zhang, W.T. Lu, F.F. Cao, Z.D. Xiao, X.S. Zheng, *J Power Sources*, 302 (2016)114.
48. S. Park, J.H. An, I.W. Jung, R.D. Piner, S.J. An, X.S. Li, A. Velamakanni, R.S. Ruoff, *Nano Lett*, 9 (2009)1593.
49. H.L. Wang, J.T. Robinson, G. Diankov, H.J. Dai, *J Am Chem Soc*, 132 (2010)3270.
50. A. Numan, M.M. Shahid, F.S. Omar, K. Ramesh, S. Ramesh, *Sensors and Actuators B: Chemical*, 238 (2017)1043.
51. J. Liang, Y. Jiao, M. Jaroniec, S.Z. Qiao, *Angew Chem Int Edit*, 51 (2012)11496.
52. M. Żyła, G. Smoła, A. Knapik, J. Rysz, M. Sitarz, Z. Grzesik, *Corrosion Science*, 112 (2016)536.
53. B.M. Chae, E.S. Oh, Y.K. Lee, *J Power Sources*, 274 (2015)748.
54. D. Bresser, E. Paillard, P. Niehoff, S. Krueger, F. Mueller, M. Winter, S. Passerini, *Chemphyschem*, 15 (2014)2177.
55. W. Liu, H. Yang, L. Zhao, S. Liu, H. Wang, S. Chen, *Electrochim Acta*, 207 (2016)293.
56. X. Wang, X.-L. Wu, Y.-G. Guo, Y. Zhong, X. Cao, Y. Ma, J. Yao, *Adv Funct Mater*, 20 (2010)1680.
57. R. Wang, C. Xu, J. Sun, Y. Liu, L. Gao, C. Lin, *Nanoscale*, 5 (2013)6960.
58. P.L. Taberna, S. Mitra, P. Poizot, P. Simon, J.M. Tarascon, *Nat Mater*, 5 (2006)567.
59. S. Hu, W. Chen, J. Zhou, F. Yin, E. Uchaker, Q. Zhang, G. Cao, *J Mater Chem A*, 2 (2014)7862.
60. K.N. Jung, S.M. Hwang, M.S. Park, K.J. Kim, J.G. Kim, S.X. Dou, J.H. Kim, J.W. Lee, *Sci Rep-Uk*, 5 (2015)7665.